Experiments on Neutron Spin Interferometry Using Spin-Echo Technique

A. I. Frank, A.V. Kozlov,

Frank Laboratory of Neutron Physics, Joint Institute for Nuclear Research, 141980, Dubna, Russia

P. Høghøj, F. Pfeiffer

Institut Laue-Langevin, Grenoble, France

G. Ehlers

HMI, Berlin, Germany.

It is well known that neutron precession in the transversal magnetic field, **B**, may be described as the manifestation of the phase difference between two components of a spinor wave function

$$\Phi = \left(\mathbf{k}_{+} \quad \mathbf{k}_{-}\right)\mathbf{x} \quad \mathbf{k}\left[\quad \frac{\mu\mathbf{B}}{\mathbf{E}}\right)^{1/2} \quad 1+\frac{\mu\mathbf{B}}{\mathbf{E}}\right)^{1/2}\Bigg]\mathbf{x}$$

$$\mathbf{F} \cong \mathbf{k}\frac{\mu\mathbf{B}}{\mathbf{E}}\mathbf{x} = \cdot\omega_{\mathrm{L}}\frac{\mathbf{x}}{\mathbf{v}}, \qquad \omega_{\mathrm{L}} \quad \frac{2\mu\mathbf{B}}{\hbar} \tag{1}$$

where μ, **B** and **E** are neutron magnetic moment, magnetic induction and neutron energy respectively, ω_{L} is the Larmor frequency and **v** is the neutron velocity. Since two components of the spinor differ by k-numbers, the result of neutron interaction with matter is as a rule not equal phase variation of the two waves. The appearance of the extra precession angle may also be interpreted as a change of the neutron travel time, Δt, caused by the sample presence, since $\Delta\mathbf{t} = \Delta\Phi/\omega_{\mathrm{L}}$. In the simplest case of the neutron passing through the sample with thickness d and the neutron refractive index **n**, it is easy to obtain

$$\Delta\mathbf{t} \cong (1-\mathbf{n})\frac{\mathbf{d}}{\mathbf{v}}, \qquad \Delta\Phi \cong \omega_{\mathrm{L}}\frac{(\mathbf{1}-\mathbf{n})\mathbf{d}}{\mathbf{v}} \tag{2}$$

These consideration were presented in references [1] regarding to the problem of the phase contrast in neutron optics. In ref. [2] the more general case of the interaction potential was discussed. In recent works [3,4] the first experimental attempts of the observation of the extra precession angle using spin-echo technique were made.

We aimed to demonstrate with better accuracy the appearances of the additional phase precession angle when neutrons pass through the refractive sample. The experiment was done at the IN15 spin-echo spectrometer [5] of the Institute Laue-Langevin, Grenoble, France. The sample was installed inside the second precession coil of the instrument which was used together with a multi-layer monocromator. We could measure precession phases for two beams of which only one passed through the sample as it shown at the fig.1.

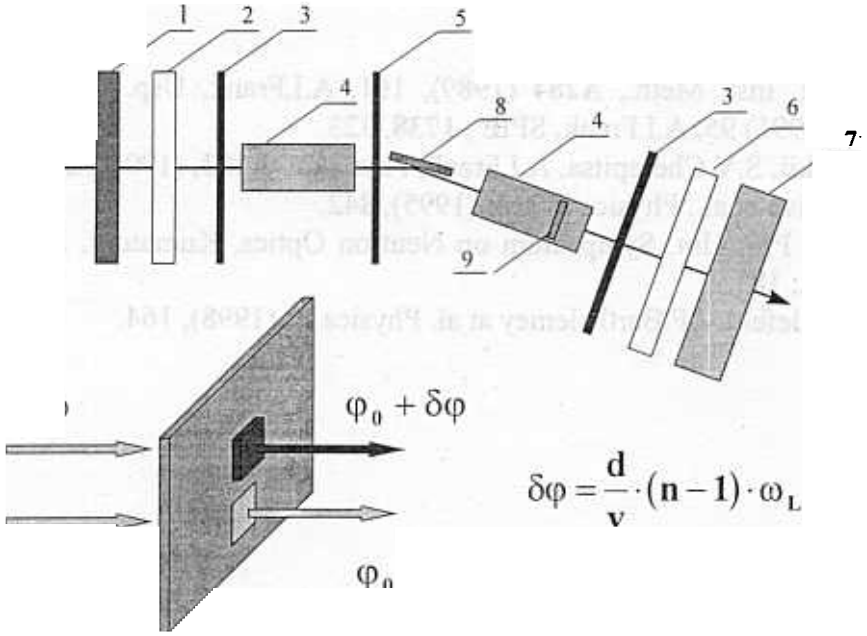

Fig.1. Scheme of the experiment. 1- velocity selector, 2- polarizer, 3- π/2 flipper, 4- precession coils, 5- π-flipper, 6- analizer, 7- position sensitive detector, 8- multi-layer monochromator, 9 - position of the diaphragm with the sample holder (shown below)

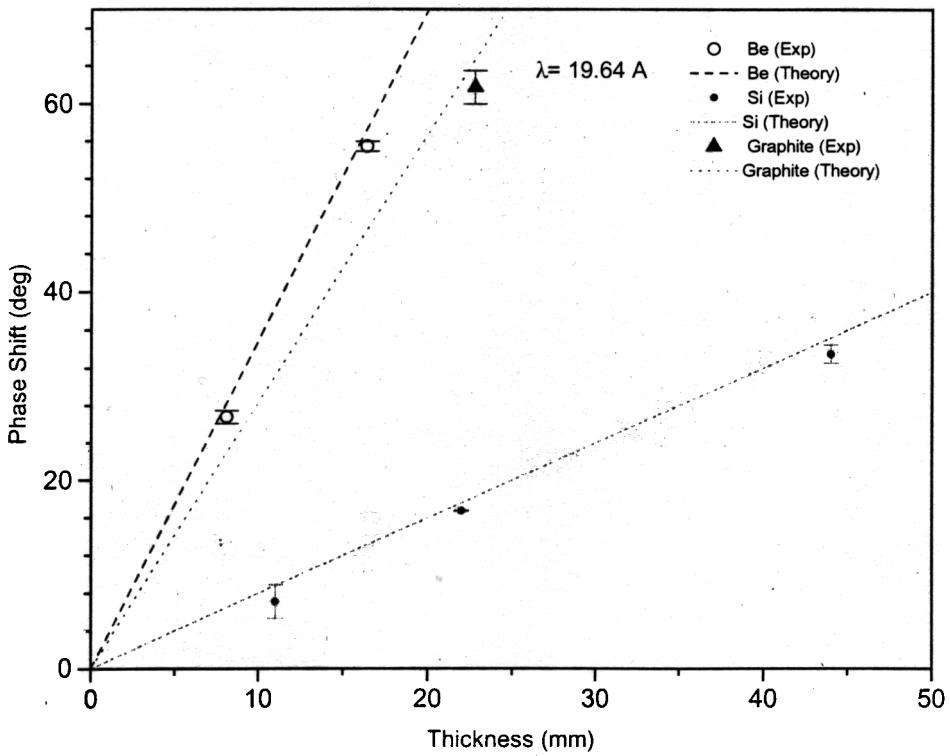

Fig.2. Measured and calculated phase precession difference between two beams.

The obtained results for the 19.6A neutrons are in an excellent agreement with theory. Similar results were obtained also with 15.5A neutrons for the Be and Si samples.

References

1. A.I.Frank, Nucl. Inst. Meth., **A284** (1989), 161, A.I.Frank, Usp. Fiz. Nauk, (Sov. Phys. Uspechy)**161** (1991) 95, A.I.Frank. SPIE , **1738**, 323.
2. V.G.Baryshevskii, S.V.Cherepitsa, A.I.Frank, Phys.Lett. **A153**, (1991), 299.
3. M.Hino, N.Achiva et.al., Physica **B 213**, (1995), 842.
4. N.Achiva et al. Proc. Int. Symposium on Neutron Optics, Kumatory. J.Phys. Soc. Jpn. **65** (1996) Suppl. A, 183.
5. P.Schleger, B.Alefeld, J.F.Barthelemey at al. Physica B, (1998), 164.

THE TECHNIQUE FOR SIMULTANEOUS ESTIMATION OF THE LEVEL DENSITY AND RADIATIVE STRENGTH FUNCTIONS OF DIPOLE TRANSITIONS AT $E_{ex} \leq B_n - 0.5$ MeV

V.A. Khitrov, A.M.Sukhovoj, E.V.Vasilieva
FLNP, JINR

Up to now the detailed and reliable information on the level density in a given J^π interval and mean probability of populating/depopulating them γ-transitions in heavy ($A > 100$) non-spherical nuclei is very pure. These parameters cannot be determined by means of traditional methods of nuclear spectroscopy from the measured spectra of γ-rays from (n_{th}, γ) reaction (or from other reactions) due to insufficient resolution of Ge detectors. The situation changed after obtaining a numerous data on the intensity distributions of the two-step cascades proceeding between the compound state and a given low-lying level. The data treatment software which allows one to derive original information from $\gamma - \gamma$ coincidences accumulated in this experiment was developed at FLNP JINR [1,2].

Using the algorithms [3,4] for analysis of $\gamma - \gamma$ coincidences registered by ordinary Ge detectors one can determine intensity distribution of cascades as a function of the excitation energy of cascade intermediate levels in the all energy region almost up to $E_{ex} \simeq B_n$ with an acceptable error which decreases as increasing an efficiency of γ-spectrometer. The measured intensity $I_{\gamma\gamma}$ of cascades is related to the unknown number of intermediate levels $n_{\lambda i} = \rho \times \Delta E$ and unknown widths of primary and secondary transitions by the relation

$$I_{\gamma\gamma} = \sum_{J,\pi} \frac{\Gamma_{\lambda i}}{\Gamma_\lambda} n_{\lambda i} \frac{\Gamma_{if}}{\Gamma_i} = \sum_{J,\pi} \frac{\Gamma_{\lambda i}}{< \Gamma_{\lambda i} > m_{\lambda i}} n_{\lambda i} \frac{\Gamma_{if}}{< \Gamma_{if} > m_{if}} \qquad (1)$$

The optimal width of interval ΔE and number N of such intervals in eq.(1) are determined by statistics of experimental data (as square of detector efficiency). A width of ΔE does not exceed 0.5 MeV even in the case of 10% efficiency detector, however. The total radiative widths Γ_λ of the capturing states are also known from corresponding experiments for all stable nuclei. The parameters $< \Gamma_{\lambda i} >$ and $m_{\lambda i}$ of the cascade γ-decay which must be found in analysis are related with the total width

$$\Gamma_\lambda = \sum_i < \Gamma_{\lambda i} > \times m_{\lambda i} \qquad (2)$$

It is clear that $N + 1$ equations (1) and (2) together with $6N$ conditions $\rho(\pi = +) > 0$, $\rho(\pi = -) > 0$, $\Gamma(E1) > 0$, and $\Gamma(M1) > 0$ restrict the interval of possible values for level density and radiative widths. This interval can be estimated with the use of two simple enough assumptions:

(a) energy dependence of level density with different J^π is determined by known and, in principle, equal for different models function;

(b) energy dependence (but not the absolute value) of widths of primary and secondary transitions is the same.

A large enough value of N, nonlinearity of eqs.(1) and (2) stipulate a choice of the way to solve the system of equations and inequalities - the Monte Carlo method. The simplest iterative algorithm was used for this aim: we set some initial values for $\Gamma(E1)$, $\Gamma(M1)$, and ρ and then distort them by means of random functions.

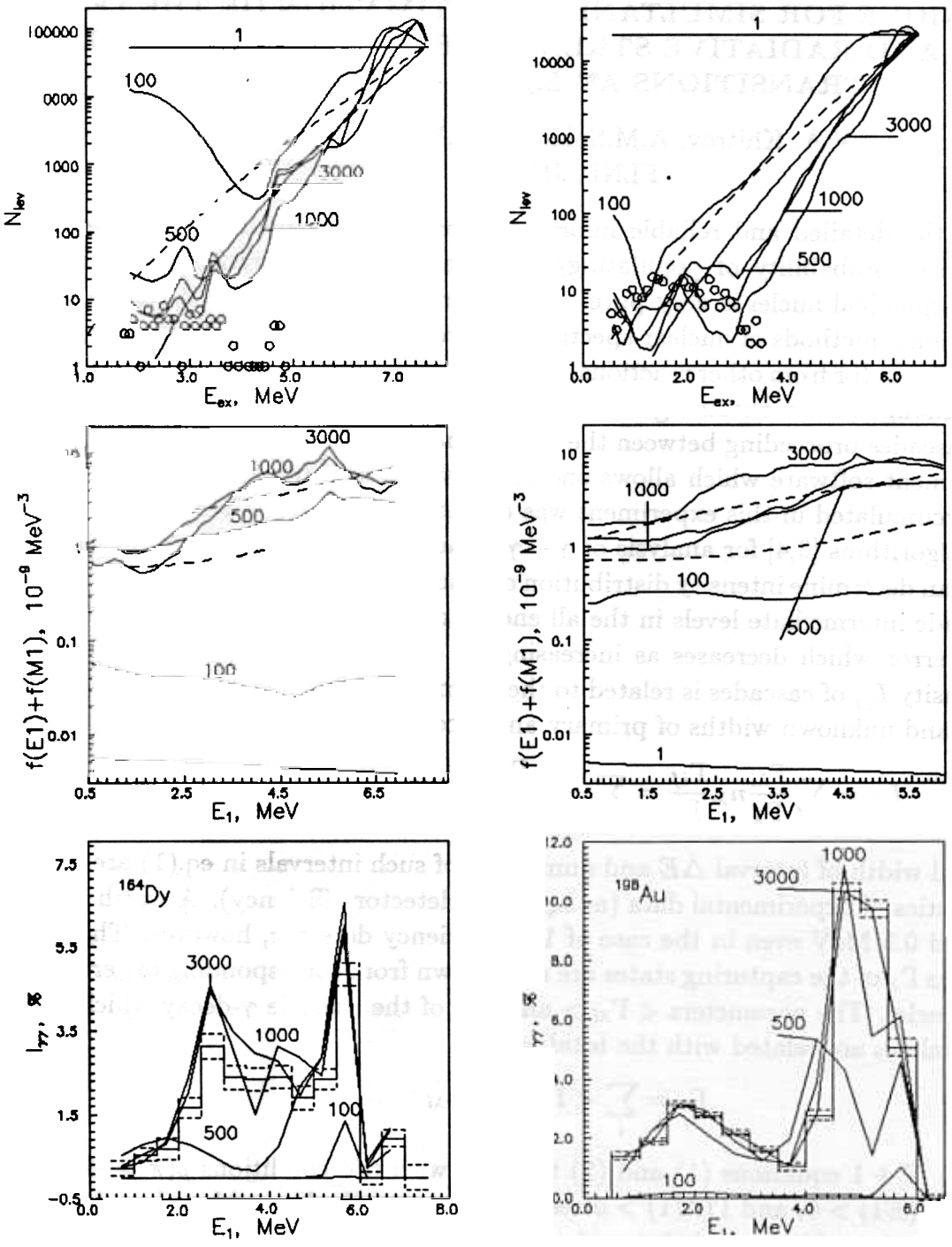

Fig. 1. The examples of the ρ and RSFs intermediate values and corresponding distributions of cascade intensities for the ^{164}Dy even-even and ^{198}Au odd-odd nuclei. Letters next to the lines mean number of iterations. Dashed curves represent predictions of the level density models [5,6] and strength function models [7,8]. Histograms show experimental cascade intensity.

If at this step of iterative procedure these distortions decrease the parameters $\Delta_1 = (I^{exp}_{\gamma\gamma} - I^{cal}_{\gamma\gamma})^2$ and $\Delta_2 = (\Gamma^{exp}_{\lambda} - \Gamma^{cal}_{\lambda})^2$ then these distorted values are used as initial parameters for the next iteration. An agreement between the experimental and calculated

cascade intensities and total radiative widths, respectively, is usually achieved after several thousands of iterations. As a result we get two random ensembles for level densities and partial widths for each of N energy intervals.

The numerous repetition of iterative calculation with different initial parameters (including obviously unreal values of Γ and ρ) for ~30 nuclei from the mass region $114 \leq A \leq 200$ showed that this algorithm gives rather narrow intervals of values for the sum level density of both parities and sum partial widths of $E1$ and $M1$ transitions. These data allow estimation of the sum radiative strength functions for $E1$ and $M1$ transitions using the following relation:

$$f = \Gamma_{\lambda i}/(E_\gamma^3 \times A^{2/3} \times D_\lambda) \tag{3}$$

The examples of intermediate results obtained within iteraive procedure for two nuclei are shown in Fig. 1. Analysis of the obtained results shows that they should be considered as probable enough estimations of level densities excited by dipole primary transitions after thermal neutron capture and radiative strength functions of these transitions. It should be noted here that no model ideas are required in this technique. Of course, the use of the reliable information on the nucleus under study decreases uncertainties of the analysis. There can be the data on energies and types of decay of known low-lying levels, mean spacings between neutron resonances, and ratio between partial widths of high-energy primary $E1$ and $M1$ transitions (although influence of two last parameters is very week).

The most critical point of the described technique is an assumption about equal energy dependence for strength functions of primary and secondary transitions. However, the assumption can be checked experimentally. This requires to measure in experiment and reproduce in calculation the intensities of two-step cascades for the maximum wide energy interval of their final level. Corresponding experiment can be realized using multidetector compton-suppressed spectrometer.

1. S.T. Boneva, E.V. Vasilieva, Yu.P. Popov, A.M. Sukhovoj,V.A. Khitrov, Sov. J. Part. Nucl. **22(2)** (1991) 232
2. S.T. Boneva et al., Sov. J. Part. Nucl. **22(6)** (1991) 698
3. Yu.P. Popov, A.M. Sukhovoj, V.A. Khitrov, Yu.S. Yazvitsky, Izv. AN SSSR, Ser. Fiz. **48** (1984) 1830
4. S.T. Boneva, V.A. Khitrov, A.M. Sukhovoj, A.V. Vojnov, Z. Phys.- A **338** (1991) 319
   S.T. Boneva, V.A. Khitrov, A.M. Sukhovoj, A.V. Vojnov, Nucl.Phys. **A589** (1995) 293
5. P. Axel, Phys. Rev. **V.126** (1962) 671
6. S.G. Kadmenskij, V.P. Markushev, W.I. Furman, Sov.J. Nucl. Phys. **V.37** (1983) 165
7. W. Dilg W. et. al., Nucl. Phys. 1973. **A217** (1973) 269
8. A.V. Ignatyuk A.V., in Proc. of IAEA Consultants meeting on the use of nulear theory and neutron nuclear data evaluation (Trieste, 1975): IAEA-190, 1976 V.1. P.211.

EXPERIMENTAL INDICATIONS OF THE PROBABLE ABRUPT CHANGE IN NUCLEAR PROPERTIES OF HEAVY NUCLEUS AT $E_{ex} \simeq 0.5B_n$

V.A. Khitrov, A.M.Sukhovoj, E.V:Vasilieva
FLNP, JINR

The cascades of two successive γ-transitions in group of nuclei from the mass region $114 \leq A \leq 200$ were studied in the framework of the program of studying nuclei with high density at FLNP JINR. Some part of the data was obtained in Riga and Rez. The observed cascades proceed between the compound state which is excited after thermal neutron capture and a group of low-lying levels. Selection of such cascades from a mass of $\gamma - \gamma$ coincidences and their analysis provided original information on nuclear properties in the excitation energy range where spacings between the levels are many times less than energy resolution of the used spectrometer.

Intensity of such cascades integrated over some interval of their intermediate levels depends on partial widths of cascade γ-transitions and number of nuclear states with $0 < E_{ex} < B_n$. A comparison between the experimental and model calculated cascade intensities shows [1] that theoretical notions of peculiarities of nuclear matter below B_n should be considerably modified. Energy dependences of level density with a given J^π and partial widths of cascade γ-transitions are the very suitable data for a comparison with the theory. The method [2,3] is developed to select the corresponding data from the cascade intensity distributions [4] built in function of the energy of the cascade intermediate levels. The results were obtained for more than 30 nuclei from the mentioned mass region.

The used data treatment software [2,3] allows one to get reliable information on the sum level density $\rho(\pi = -) + \rho(\pi = +)$ excited by $E1$ and $M1$ primary transitions and sum of their radiative strength functions $f(E1) + f(M1)$. Uncertainties of $\rho(\pi = -)$ and $\rho(\pi = +)$ as well as $f(E1)$ and $f(M1)$ separately are noticeably larger than those for corresponding sum values. It should be noted that the technique [2,3] does not use model ideas of process under study (except the shape of spin dependence of level density) and is very sensitive to minimum density of excited states. There are two most considerable differences of our technique [2,3] from known methods [5] to derive level density from the spectra obtained in the neutron induced nuclear reactions. Also, there were no methods up to now which determined strength functions for primary transitions populating the levels of heavy enough nuclei at the energy of some MeV.

The main result of the analysis [2,3] that both traditional and modern enough ideas of a nucleus at excitations from 1-3 MeV to B_n need serious corrections. Discrepancy between the level density observed by us in the (n_{th}, γ) reaction (at least in the case of the two-step cascades) and predictions of the Fermi-gas level density model which considers nucleus as a system of noninteracting fermions testifies to considerable role of phonon excitations in the wave functions of the observed states. (We do not introduce some new ideas of nuclear matter even for qualitative explanation of our results but use simple known notions). The more modern models like the generalized model of the superfluid nucleus [6,7] provides better agreement with the experimental level density, however even in this case discrepancy exceeds experimental uncertainties.

A comparison between the results [2,3] and model calculations allowed one more essential conclusion: energy dependence of level density at $E_{ex} \simeq 3-4$ MeV exhibits more or less clearly expressed "step" (see Fig. 1.). The conclusion is in complete agreement with the results [8] of approximation of random fluctuations of the cascade intensities relative to their mean value which provided estimation of the total number of levels which can be excited in the (n_{th}, γ) reaction below 3-4 MeV.

Complete explanation of the observed [2,8] effect is possible only in the framework of the strong nuclear model which reproduces experimental level density with experimental precision. However, the most probable qualitative explanation can be suggested under assumption that the thermodynamical function — specific heat of nuclear matter in the total energy region of excitation where the second order phase transition can affect nuclear properties — has the same functional dependence on energy as that which is known for a mixture of superfluid ^3He and ^4He. A well known fact of increase in specific heat of quantum liquid in the region of the second order phase transition can signify decrease in nuclear temperature and, as consequence, level density of fermion-type at certain nuclear energy. Because energy dependence of level density is exponential for both fermions and bosons then the presence of "step" requires one to postulate that at the excitation energy of several MeV in heavy nucleus the number of phonons is noticeably less than the number of quasiparticles but energy of bosons considerably exceeds energy of fermions. Such assumption follows from proportionality of the parameter a (which determines level density) to the number of excited quasiparticles or phonons. I. e., adiabatic principle – one of the basic principle of the generalized model of the superfluid nucleus – is not fulfilled. The BCS-theory [9] predicts the transition of Fermi-liquid to Fermi-gas at temperature

$$T_c \quad \frac{\delta}{1.76}, \tag{1}$$

what is approximately two times higher than the point of abrupt change in level density in our experiment. This fact can be easily explained if one take into account a decrease in temperature of phase transition in mixture of liquid ^3He and ^4He as compared with pure ^4He. Probably, more correct variant of the model of the superfluid nucleus must take into account this temperature shift, i. e., consider nucleus as a mixture of boson and fermion excitations in the wide energy interval.

The presence of phonon excitations strongly affecting nuclear properties appears as two more effects observed when studying two-step cascades:

(a) approximate harmonicity in the excitation spectra of intermediate levels (or their groups) of most intense cascades:

(b) noticeable increase in strength functions (i. e., intensities of cascade transitions) as compared with the model [10] which considers nucleus as a drop of Fermi-liquid. The estimated from the experiment and calculated according to conventional models strength functions are shown in Fig. 2. As can be seen from figure, the maximum values of the sum strength functions of $E1$ and $M1$ transitions are observed at $\sim B_n$, i. e., they conform to the energy of "step" in our level density.

So, the analysis of totality of experimental data on the two-step cascades leads to conclusion about probability of abrupt enough change in nuclear properties at $E_{ex} \simeq 3-5$ MeV and necessity of serious correction of corresponding nuclear models.

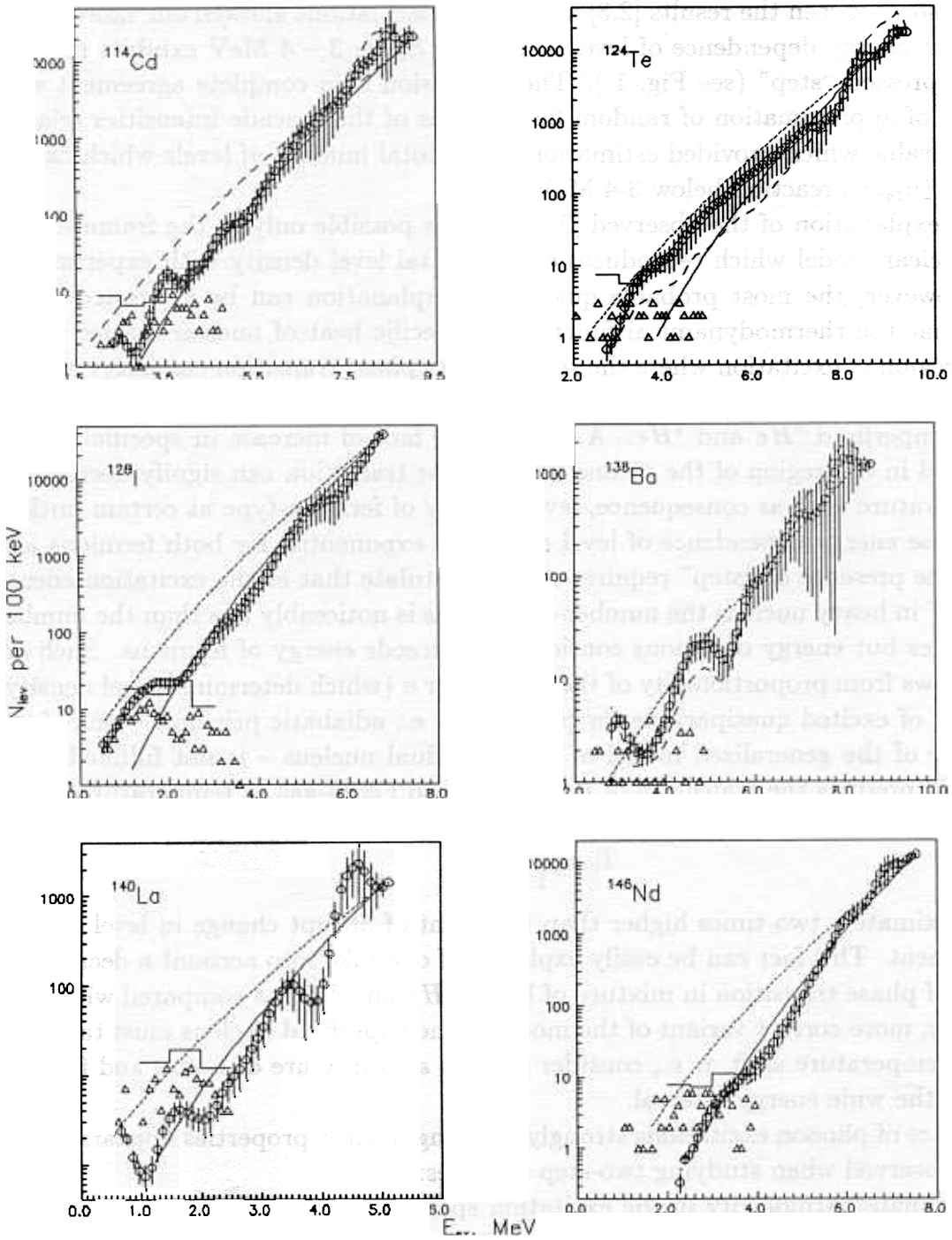

Fig. 1. The numbers of levels of both parities with errors (circles with bars) for ^{114}Cd, ^{124}Te, ^{128}I, ^{138}Ba, ^{140}La, and ^{146}Nd. Histogram - - data [8], triangles —experimental level density from the $(n, 2\gamma)$ reaction. Dashed line - · the ρ value obtained at the unreal initial parameter $\rho(E_{ex}) = \rho(B_n)$ of iterative process. The upper and lower curves represent predictions of models [11] and [7], respectively.

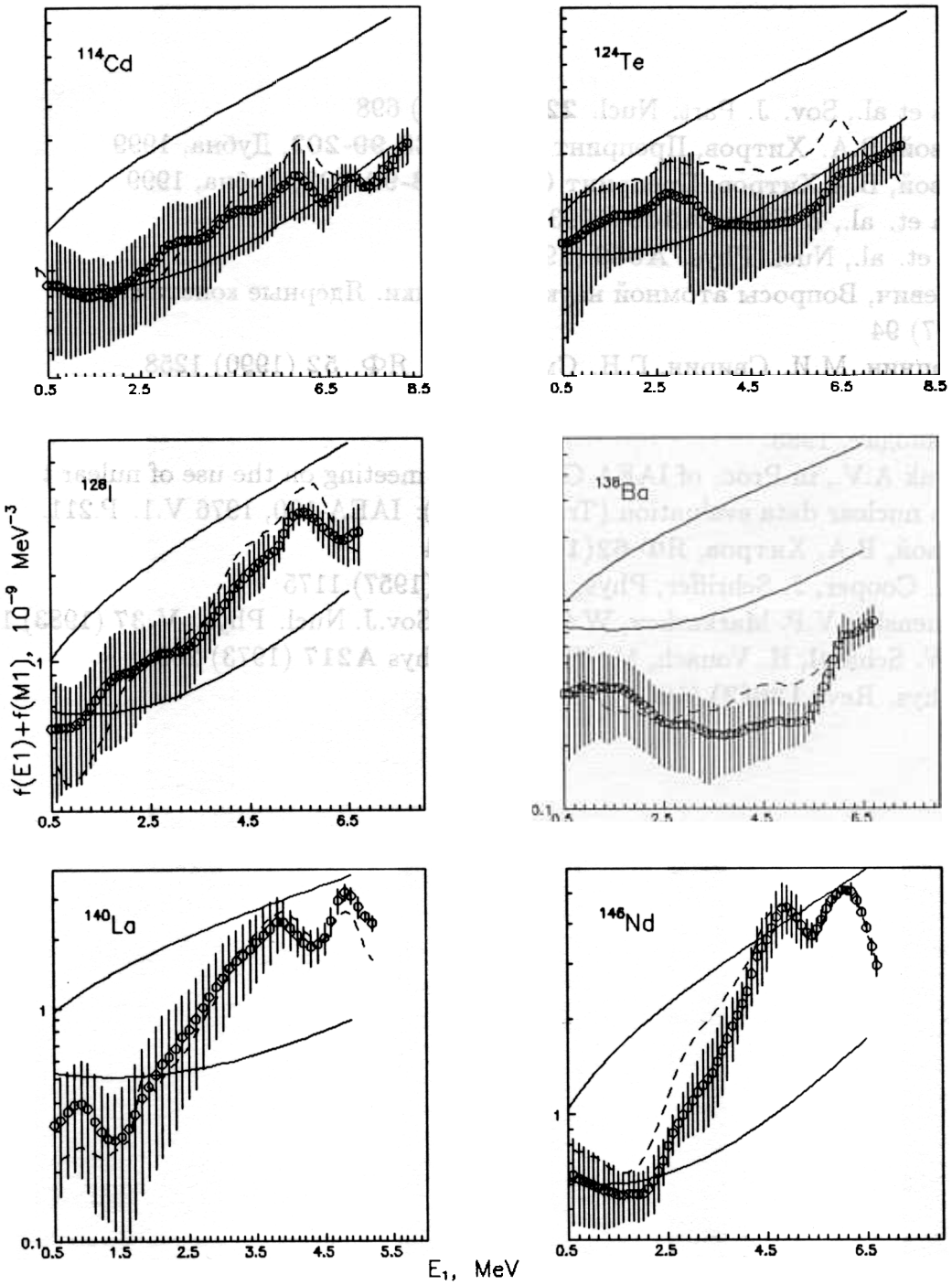

Fig. 2. The sum of the probable radiative strength functions of $E1$ and $M1$ transitions (with estimated errors) in the ^{114}Cd, ^{124}Te, ^{128}I, ^{138}Ba, ^{140}La, and ^{146}Nd nuclei. Dashed curve represents the $f(E1) + f(M1)$ mean value obtained at different initial values of strength functions and at initial level density $\rho(E_{ex}) = \rho(B_n)$ with the help of iterative procedure. Upper and lower solid curves represent predictions of models [12] and [10], respectively.

References

1. S.T. Boneva et al., Sov. J. Part. Nucl. **22(6)** (1991) 698
2. А.М. Суховой, В.А. Хитров, Препринт ОИЯИ, **Е3-99-202**, Дубна, 1999
3. А.М. Суховой, В.А.Хитров, Препринт ОИЯИ, **Е3-99-203**, Дубна, 1999
4. S.T. Boneva et. al., Z. Phys. **A346** (1993) 35
   S.T Boneva et. al., Nucl. Phys. **A589** (1995)293
5. О.Т. Грудзевич, Вопросы атомной науки и техники. Ядерные константы. **В.3-4** (1997) 94
6. Е.М. Растопчин, М.И. Свирин, Г.Н. Смиренкин, ЯФ. **52** (1990) 1258
7. А.В. Игнатюк, Статистические свойства возбужденных атомных ядер, М., Энергоатомиздат, 1983.
   A.V. Ignatyuk A.V., in Proc. of IAEA Consultants meeting on the use of nulear theory and neutron nuclear data evaluation (Trieste, 1975): IAEA-190, 1976 V.1. P.211.
8. А.М. Суховой, В.А. Хитров, ЯФ **62(1)** (1999) 24
9. J. Bardin L. Cooper, J. Schriffer, Phys. Rev. **108** (1957) 1175
10. S.G. Kadmenskij, V.P. Markushev, W.I. Furman, Sov.J. Nucl. Phys. **V.37** (1983) 165
11. W. Dilg, W. Schantl, H. Vonach, M. Uhl, Nucl. Phys **A217** (1973) 269
12. P. Axel, Phys. Rev. **126(2)** (1962) 671

NEW METHOD OF PARTIAL RADIATIVE CAPTURE CROSS SECTION MEASUREMENTS

Yu.P.Popov, A.V.Voinov, P.V.Sedyshev, S.S.Parzhitski, A.P.Kobzev, N.A.Gundorin, D.G.Serov, M.V.Sedysheva.

New method is based on the measurements of the energy shift of the primary γ-transition due to the capture of intermediate neutron with respect to its position after the thermal neutron capture. If an intense of the primary γ-transition with the energy $E^i_{\gamma 0}$ to the i-th final level of the excited nucleus after a thermal neutron capture ($E_n \cong 0$) by a nucleus with the atomic weight A, the energy of the γ-transition following the capture of an neutron with energy E_n must be:

$$E^i_\gamma = E^i_{\gamma 0} + A/(A+1)E_n$$

The method was first demonstrated in [1], where two resonances of sulfur were registered by using of reactor neutron beam with boron filter. However the authors did not manage to derive any information from the experiment beside the experimental widths of two resonances.

In our case the neutrons in the energy interval about 10 – 120 keV were generated by ^{7}Li(p,n) reaction by the Van de Graaff accelerator at proton energy exceeding the reaction threshold by ΔE_p =60 keV.

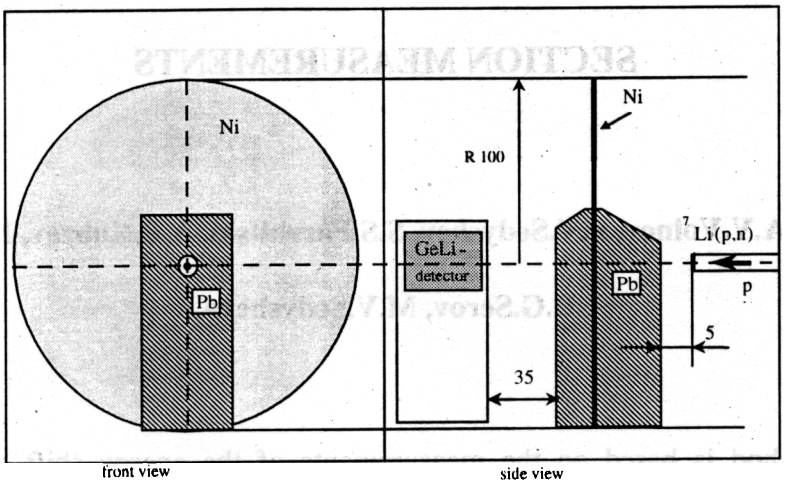

Fig. The draft of the experimental setup. The dimensions are in mm.

The draft of the experimental setup is shown in Fig. This compact geometry provided the optimum for efficiency of the γ-quanta registration and for irradiation of the sample by neutrons. According to the background measurements (without sample or with scatterer of pure graphite) the main components of background are due to the Compton effect in Ge-detector from Fe(n,γ) reaction on constructive materials (including on the turning magnet of the proton beam).

At first step of this method development we used the samples of Fe [2] and Ni [3], where the partial γ-transitions for several most intensive resonances was investigated by another methods [4,5]. It gives us possibility to standardize our relative cross sections data and check the new method.

For illustration of the method the part of experimental γ-quanta spectrum for Ni sample is presented on fig.2. One can see the structure in the spectrum due to $^{58}Ni(n,\gamma_0)^{59}Ni$ reaction with population of ground state of ^{59}Ni nucleus. Left peak belongs to the thermal neutron

capture and indicates the zero position of the neutron energy scale. The other peaks are due to the resonance neutron capture.

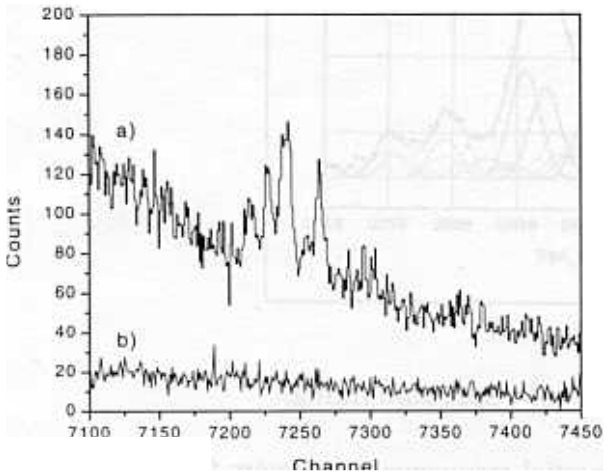

Fig.2. The experimental spectrum of $^{58}Ni(n,\gamma_0)^{59}Ni$ reaction with resonance neutrons produced by $^{7}Li(p,n)$ reaction with ΔE_p=60 keV over the reaction threshold (a), the background spectrum (b).

The experimental γ-quanta spectrum for the Fe sample is presented on the fig.3. The first two peaks are due to the thermal neutron capture by ^{56}Fe nucleus with population of ground and first excited state of ^{57}Fe. The counts to the right of the doublet are due to the γ-transitions populating these two states for the resonanse neutron capture. 16 γ-transitions (2 γ-transitions for 1 s-wave neutron resonance (27.7 keV) and 14 γ-transitions for 7 known p-wave resonances) may give the contribution to the resonance bump. For s-wave resonance these γ-transitions have E1 multipolarity, for p-wave they have M1 multipolarity. The fitting procedure (see Fig.3) and the data analysis method are described in [2].

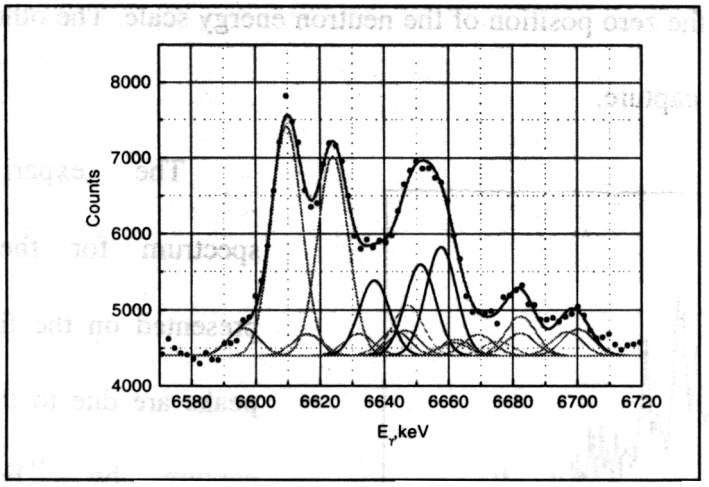

Fig.3 Graphical results of γ-spectrum fitting.

For absolute nornalization we used the known partial resonance parameters from [4,5]. Since the individual γ-transitions could overlap, we have determined only the partial radiative widths of the M1 multipolarity averaged over 7 p-wave resonances: $<\Gamma_{\gamma i}>$=69 meV.

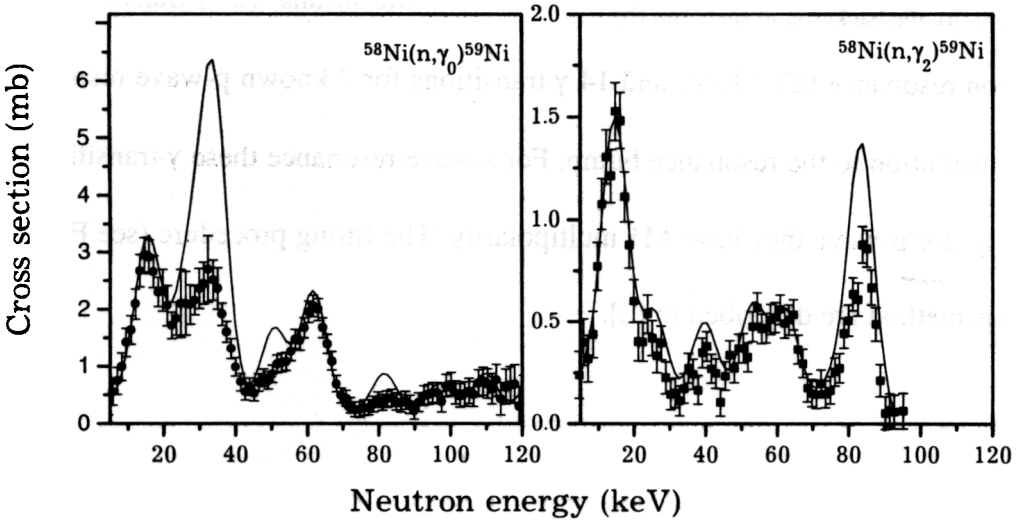

Fig.4. The partial cross sections of $^{58}Ni(n.\gamma_0)^{59}Ni$ (left) and $^{58}Ni(n.\gamma_2)^{59}Ni$ (right) reaction. The points are represented the experimental data and does not take into accounts the correction coefficients conjuncted with self-absorption and multiple scattering of neutrons in the sample. Full line are shown the corrected cross section.

The one of the first results obtained for ^{58}Ni isotope is shown in the Fig.4 where the partial cross section of ^{58}Ni(n,γ)^{59}Ni reaction for population of both the ground and second excited states of ^{59}Ni is presented. Each peak in the structure of the partial cross section is due to the contribution of a single resonance or group of the resonances. It allowed us with help of the fitting procedure to derive the partial parameters of neutron resonances and by using the partial values of radiative widths [4] make absolute normalization of our partial cross section data. It should be underlined that this result is obtained for the first time because of the high efficiency of this method in comparison with others.

New method developed in FLNP for measurements of the partial capture cross sections in the keV neutron energy region possess the record efficiency. It gave the possibility to receive the results unattainable now for the time-of-flight method not only for van de Graaff neutron sources but for the modern powerful neutron sources on the base of electron and proton accelerators. The energy dependence of the partial neutron capture cross sections was measured for the first time.

V.J.Thomson, A.V.Lopez.W.V.Prestvich, T.J,Kennett, Nucl. Instr. Meth.**126**,(1975) 263

2. Yu.P.Popov, P.V.Sedyshev, A.P.Kobzev, S.S.Parzhitski, N.A.Gundorin, D.G.Serov, M.V.Sedysheva. Phys. At. Nucl. **62** (1999) 827-831
3. Yu.P.Popov, A.V.Voinov, P.V.Sedyshev, A.P.Kobzev, S.S.Parzhitski, N.A.Gundorin, D.G.Serov. In: ISINN-7, Dubna 1999 (JINR, Dubna, 1999) 214-218.
4. H. Beer, R.R.Spenser, F.Kaeppeler, Z.Phys. A**284**, (1978) 73
5. H.Komano, M.Igashira, M.Shimizu, H.Kitasava, Phys.Rev. C**29,** (1984) 345

DETERMINATION OF THE FORWARDBACKWARD ASYMMETRY COEFFICIENT IN $^{35}Cl(n,p)^{35}S$ REACTION

Yu.M.Gledenov, R.Machrafi, A.I.Oprea, P.V.Sedyshev, V.I.Salatski, P.J.Szalanski
Joint Institute for Nuclear Research, 141980 Dubna, Russia

In the frame of mixing states with different parities model, the forward-backward α_{FB}, left-right α_{LR} and parity non-conservation α_{PN} asymmetry coefficients in the (n,p) reaction play an important role, because as is indicated in [1] the weak matrix element can be written like an expression of these three coefficients. So, in principle, if it is realized one experiment (or more) for measuring these coefficients it will be possible to obtain the weak matrix element. Recently, with resonance neutrons (up to 1keV) of the pulsed reactor IBR-30, Frank Laboratory of Neutron Physics, JINR, Dubna, it has been carried out an experiment for measuring the forward backward coefficient asymmetry on the NaCl target. Theoretically, the maximum of this coefficient is expected around E_n= 288 eV. The values of the α_{FB} have been obtained in different neutron energy intervals: 0.5-10, 150-260 and around the resonance (E_n=398 eV).

The experiment has been carried out at the 31m path of the pulsed reactor IBR-30. The neutron spectroscopy was performed by the time of flight method. It has been used a double section ionization chamber [2]. In one of its section was fixed a NaCl target of 0.5 mg/cm^2 and 200 mm in diameter onto 100 μm aluminum backing. The chamber was filled up with Ar + 4% CO_2 gas mixture at the pressure 0.35 ata. The pulse-height and time of flight spectra were registered using a multiparameter data acquisition system. The chamber has been periodically turned at 180^0 from its previous position, in one position we have measured the forward effect, while in the second position it has measured the backward effect. To normalize the neutron flux, we have used a boron counter monitor. The scheme of our experiment is shown in Fig.1.

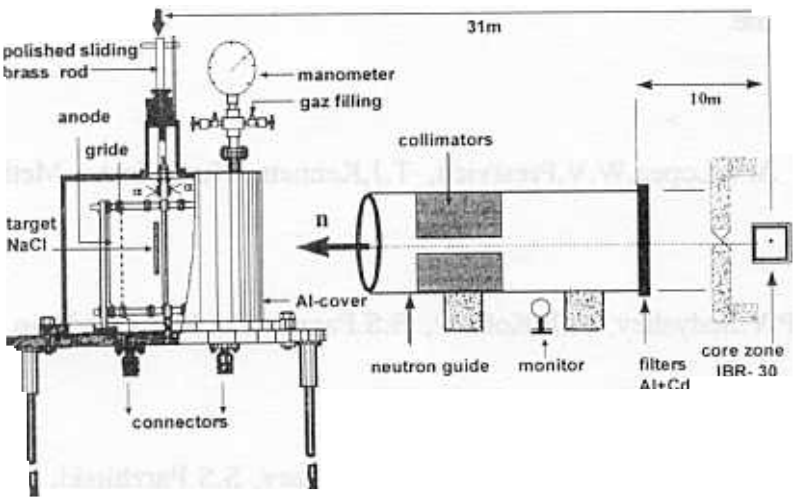

Fig.1. Experimental setup of the forward-backward asymmetry coefficient measurement

The forward-backward asymmetry coefficient was determined by the formula:

$$\alpha_{FB} = \frac{N_F - N_B}{N_F + N_B} \qquad (2)$$

Where, N_F – is the number of registered protons emitted in the forward direction, N_B – the number of registered protons emitted in the backward direction. The neutron energy dependence

of the $^{35}Cl(n,p)^{35}S$ reaction cross section is shown in Fig.2a. The theoretical evaluation of the forward-backward coefficient up to 2 keV is given in Fig.2b [3].

In Fig.3a and Fig.3b are shown the pulse-height spectra obtained in the neutron energy ranges 0.5-10 eV and 150-260 eV, while the Fig.3c illustrates a part of the time of flight spectra in the resonance region.

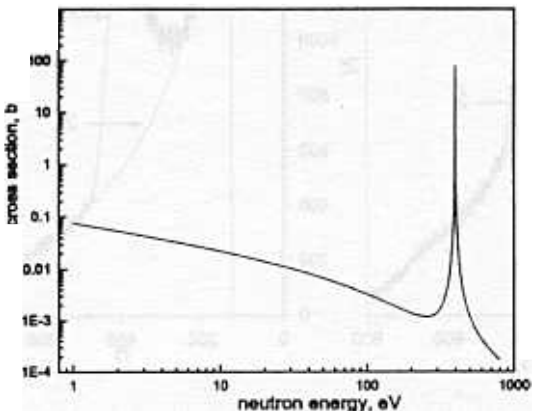

Fig.2a. The energy dependence of the $^{35}Cl(n,p)^{35}S$ cross section

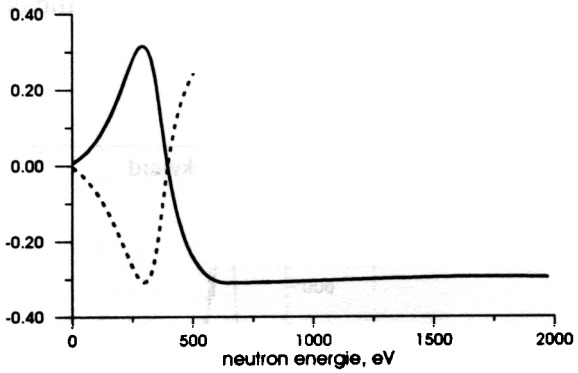

Fig.2b. Energy dependence of the forward backward asymmetry coefficients

The proton yields N_F and N_B have been obtained by the separation of the effect from the background on the pulse-height spectrum (Fig.3a and Fig.3b) for the neutron energy intervals 0.5-10 eV and 150-260 eV. But in the resonance region the value of the α_{FB} has been determined from the time spectrum shown in Fig.3c. The table 1 shows the obtained results.

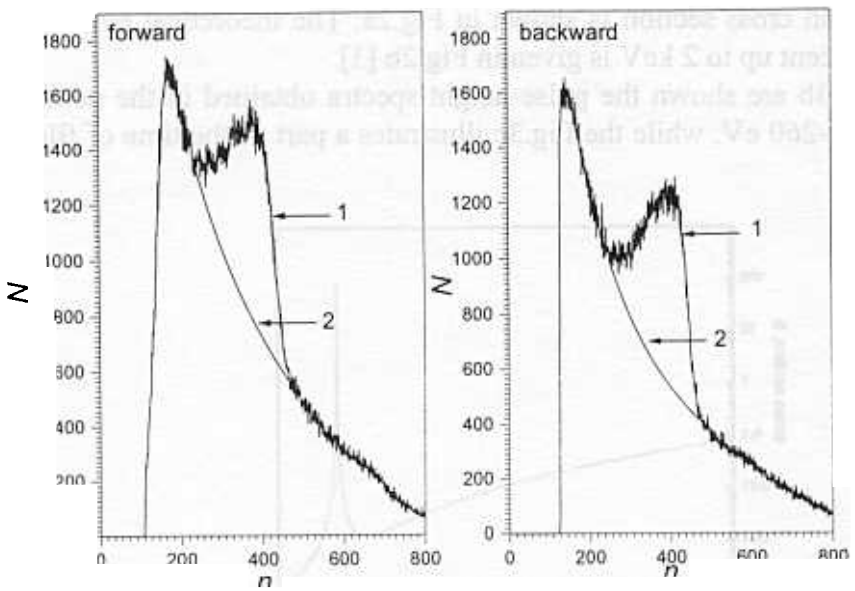

Fig.3a. The pulse height spectrum obtained in 0.5-10 eV, 1-event + background, 2- background, n- is the channel number, N- is the count per channel

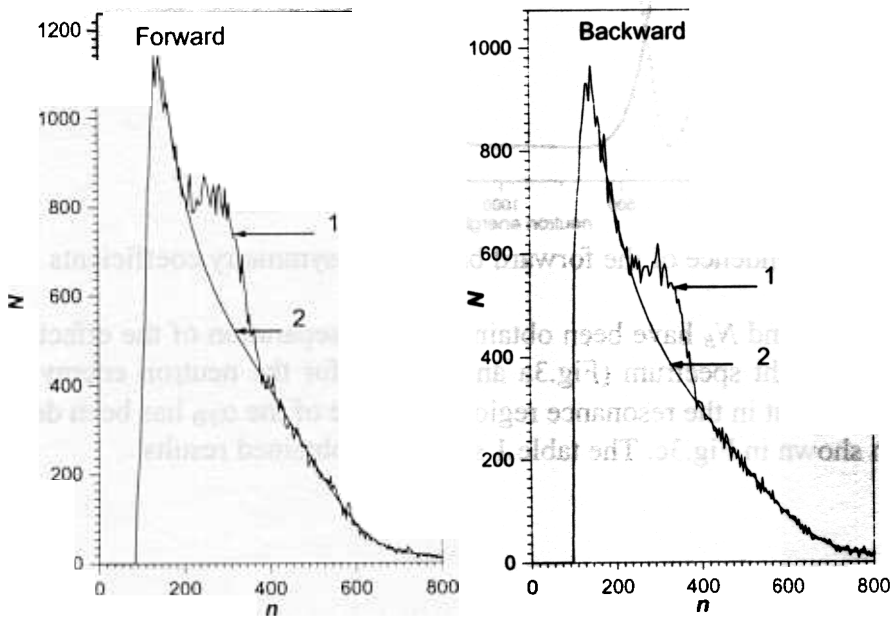

Fig.3b. The pulse height spectrum obtained in 150-260 eV, 1-event + background, 2- background, n- is the channel number, N- is the count per channel

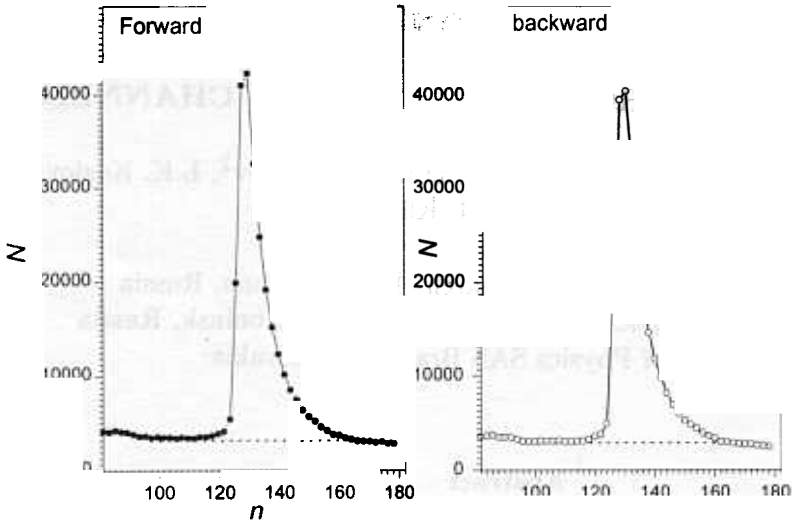

Fig.3c. Part of the time of flight spectrum for the forward backward in the resonance region n- is the channel number, N- is the count per channel

Table 1. The experimental results of the forward-backward asymmetry coefficient

The neutron energy range ,eV	$\bar{E}$,eV	α_{FB}
0.5 - 10	5.2	0.030 ± 0.005
150 - 260	205	0.17 ± 0.03
resonance region	398	0.002 ± 0.006

Using the parity non-conservation coefficient α_{PN} =-1.51x10^{-4}, the left-right α_{LR}=-2.4x10^{-4} coefficients at the thermal point energy and the forward-backward asymmetry coefficient α_{FB} = 0.17 [4,5], we obtain for the weak matrix element M_{PV}=57±17 meV.

References

[1]. Zenkin S.V., Titov N.A. Preprint INR RAS П-0367, Moscow (1984)
[2]. Yu.M.Gledenov, G.Khuukhenkhuu, M.V.Sedysheva et al., JINR Communication, E3-95- 445, Dubna (1995)
[3]. Yu.M.Gledenov, A.I.Oprea, V.I.Salatski, P.V.Sedyshev, P.I.Szalansky, Asymmetry coefficient in (n,p) reactions ISINN-6 Dubna, 1998
[4]. Yu.M.Gledenov et al., Nuclear Phys. A654 (1999) 943c-948c
[5]. A.Antonov, V.A.Vesna, Yu.M.Gledenov et al. Pis'ma ZETF. 40 (1984) 209.

ANGULAR ANISOTROPY OF FISSION FRAGMENTS FROM THE RESONANCE NEUTRON INDUCED FISSION OF ALIGNED ^{235}U TARGET AND THE ROLE OF $J^{\pi}K$ FISSION CHANNELS

Yu.N. Kopatch[1] A.B. Popov[1], W.I.Furman[1], D.I. Tambovtsev[2], L.K. Kozlovsky[2], N.N. Gonin[2], and J. Kliman[1,3]

[1]Joint Institute for Nuclear Research, 141980 Dubna, Russia
[2)]SSC Institute of Physics and Power Engineering Obninsk, Russia
[3)]Institute of Phvsics SAS Bratislava, Slovakia

Abstract

Energy dependence of the fission fragment angular anisotropy from $^{235}U(n,f)$ reaction has been measured by the FLNP-IPPE collaboration using the JINR pulsed neutron source IBR-30. Our data are analyzed together with the total neutron, total fission and spin-separated fission cross sections in energy range $0 - 30$ eV in order to obtain a new set of s-wave resonance parameters. Three fission channels ($K = 0, 1, 2$) are taken into account for both spin groups, $J = 3^-$ and $J = 4^-$. The obtained set of resonance parameters is discussed. Integral distributions of partial and total fission widths are compared with the Porter-Thomas distributions. Estimation of the degrees of openness of different $J^{\pi}K$ fission channels is made. A problem of ambiguity of the resonance parameters is also briefly discussed.

1. Fission induced by slow neutrons is one of the unique tools for studying the quantum-mechanical aspects of the fission process. It gives a possibility to obtain information about the fission amplitudes $\gamma_{f\lambda}^{J^{\pi}K}$ for a given resonance λ. These parameters form a basis for a quantitative description of the fission process induced by resonance neutrons. Here, $J^{\pi}K$ are the spin, parity and the spin projection onto the symmetry axis of the fissioning nucleus. It is known [1, 2] that such amplitudes cannot be extracted unambiguously using only data on integral fission and neutron cross sections. Additional information can be obtained from experiments on the interaction of polarized (or unpolarized) neutrons with a polarized (aligned) target.

We performed an experimental study of the energy dependence of the differential fission cross section (fission fragment angular anisotropy) of ^{235}U resonance neutron induced fission using an aligned target and unpolarized neutrons.

2. The experiment has been performed at the booster IBR-30 + LEA-40 in Dubna and is a development of the technique used by Pattenden and Postma.[3] The detailed description of the experimental set-up and of the primary data analysis can be found in.[4, 5]

The energy dependence of the A_2 coefficient, which characterizes the angular anisotropy of fission fragments, is shown in fig. 1.

For a combined analysis, we used the experimental cross sections for ^{235}U available from the National Nuclear Data Center (NNDC) at BNL.[6] The data sets selected for the analysis are summarized in Table 1.

3. The experimental data sets listed in Tab. 1 were fitted over the energy region $0 - 30$ eV using the standard R-matrix formalism in the Reich-Moore approximation [13] with the inclusion

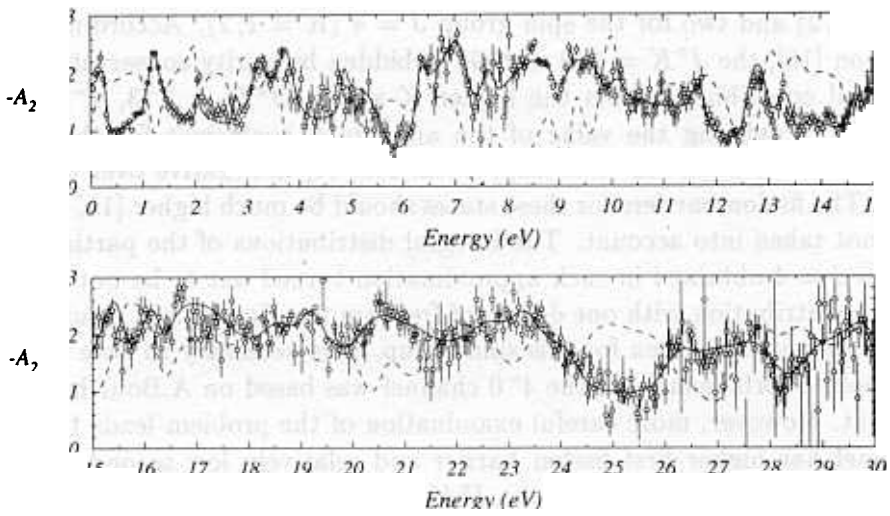

Figure 1: The results of the fit (solid curve) for $A_2(E)$, circles are experemental data. Dashed line is calculated using the resonance parameters from.[13]

of formulae for $A_2(E)$ derived in ref. [14] (see also for details ref. [5]). In the fit, each resonance λ was described by six resonance parameters: E^λ, Γ_γ^λ, γ_n^λ, γ_f^λ, ϕ^λ, and θ^λ. Such parameterization allows one to include up to 3 fission channels for each resonance λ. The partial fission amplitudes are expressed via the module of the total fission amplitude $\gamma_f^\lambda = \sqrt{\Gamma_f^\lambda}$ and two angles, ϕ^λ and θ^λ, in a spherical coordinate system:

$$\gamma_{f1}^\lambda = \gamma_f^\lambda \cdot \cos\phi^\lambda \cdot \sin\theta^\lambda, \quad \gamma_{f2}^\lambda = \gamma_f^\lambda \cdot \sin\phi^\lambda \quad \sin\theta^\lambda \quad \gamma_{f0}^\lambda = \gamma_f^\lambda \cdot \cos\theta^\lambda \tag{1}$$

Table 1: The experimental data sets selected for the evaluation

	Type of cross section	**Authors**	**Energy range**
1	$A_2(E)$	Present work	0.06 – 30 eV
2	Fission (σ_{nf})	R.Gwin et al.[7]	0.0016 – 9.7 eV
3	Fission (σ_{nf})	L.W.Weston et al.[8]	9.7 – 30 eV
4	Spin-separated fission (σ_{nf}^J)	V.L.Sailor et al.[9]	0.075 – 1.14 eV
5	Spin-separated fission (σ_{nf}^J)	M.S.Moore et al.[10]	1.6 – 30 eV
6	Total (σ_{ntot})	F.D.Brooks et al.[11]	0.035 – 1.3 eV
7	Total (σ_{ntot})	A.Michaudon et al.[12]	1.3 – 30 eV

The radiative width Γ_γ^λ was fixed and equals 0.039 eV for all resonances. All other parameters were varied. First we analyzed the data assuming that three channels are open for the spin group

$J = 3$ ($K = 0, 1, 2$) and two for the spin group $J = 4$ ($K = 1, 2$). According to the commonly used assumption [16], the $J^\pi K = 4^-0$ state is forbidden by parity conservation. We can expect no or very small contribution from the higher K states ($J^\pi K = 3^-3$, 4^-3, and 4^-4) as the geometrical factors defining the value of the anisotropy coefficient for these states have the positive sign while the observed anisotropy coefficient A_2 is negative over the whole measured energy range. The fission barriers for these states should be much higher [15, 16]. So these fission channels are not taken into account. The integral distributions of the partial fission widths for the spin group $J = 4$ obtained in such approximation turned out to be not consistent with the Porter-Thomas distribution with one degree of freedom (see fig. 3, right column). An additional fission channel seems to be open for this spin group. It is necessary to note that the conclusion [16] about absolute forbidenness of the 4^-0 channel was based on A.Bohr hypothesis [15] in its simplest variant. However, more careful examination of the problem leads to a conclusion that the 4^-0 channel has higher first fission barrier and relatively low second one for asymmetric fission modes. Thus, one would expect the $J^\pi K = 4^-0$ channel to be at least partially open for our case. So we reanalyzed the data assuming that all three channels are open for both spin groups.

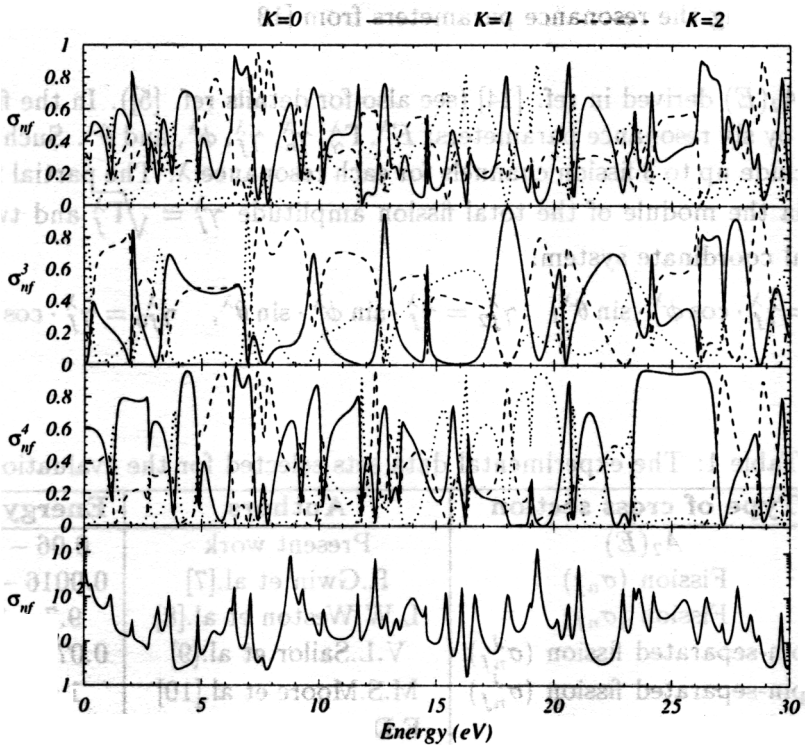

Figure 2: Decomposition of the total and spin-separated fission cross sections into K components. Energy dependence of the total fission cross section is shown in the lower plot.

The results of the final fit for $A_2(E)$ are shown in fig. 1 All other cross sections are also

well reproduced. The dashed line is calculated using a set of resonance parameters from the ENDF/B-VI library [13] which also describes all other cross sections quite well, but obviously fails to reproduce the A_2 energy dependence. It is necessary to note that the latter set of resonance parameters was obtained in the two channel approximation and without taking into account the information on $A_2(E)$.

4. Figure 2 shows the relative contributions of different K-components to the total and spin separated fission cross sections. As is expected, there are large fluctuations of weights of the K-channels for different compound states λ which result in the strong fluctuations of the relative K-contributions. It can be noted that the contribution of the $K = 0$ component is significant both in the spin-separated and the total fission cross sections.

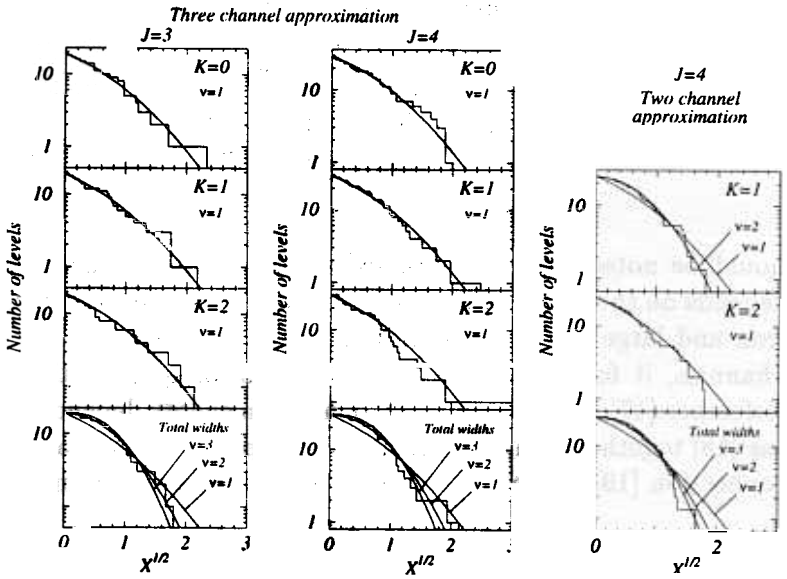

Figure 3: Integral distributions of partial and total fission widths (number of resonances with $\Gamma_{\lambda f}/\langle\Gamma_{\lambda f}\rangle > X$). Solid lines are the χ^2 distributions with ν degrees of freedom.

The integral distributions of the partial and total fission widths of resonances in the energy interval 0 – 30 eV are given in fig 3 (left and middle). The experimental distributions for each separate $J^\pi K$ channel are in good agreement with the Porter-Thomas distribution with one degree of freedom. The integral distributions of the total fission widths for both channels also fluctuate according to the Porter-Thomas distribution with the number of degrees of freedom being between 2 and 3.

The average partial ($\langle\Gamma^\lambda_{f,K}\rangle$) and total ($\langle\Gamma^\lambda_f\rangle$) fission widths for each fission channel are listed in Tab.2. The average contributions of different fission channels, defined as

$$W_K = \frac{1}{N_\lambda}\sum_\lambda \frac{\Gamma^\lambda_{f,K}}{\Gamma^\lambda_f} \qquad (2)$$

which can be regarded as a measure of the degree of openness of a given channel are shown in Tab.3. One can see that these values are almost equal for both spin groups. The $K = 0$ channel seems to be somewhat suppressed, which is consistent with modern theoretical considerations.

Table 2: Average partial and total fission widths in meV

	K=0	K=1	K=2	Total
J=3	35.0	68.1	74.0	177.1
J=4	20.4	34.0	38.0	92.4
J=3+4	26.1	47.2	51.9	125.2

Table 3: Degrees of openness of different fission channels (%)

	K=0	K=1	K=2
J=3	25	39	35
J=4	26	40	34
J=3+4	26	40	34

Finally, it should be noted that the obtained set of resonance parameters is not uniquely determined. It depends on the choice of negative resonances as well as on inclusion of resonances with small neutron and large total fission widths. However, since this parameter set includes all possible K channels, it forms the most reliable basis for quantitative analysis of $s-$ and $p-$resonance interference.[17] A combined study of neutron energy dependence of fragment mass-TKE distributions [18] together with an angular anisotropy coefficient can give new information about the interconnection [19] of the Bohr fission channels and fission modes.

References

[1] G.F.Auchampaugh, *Nucl. Phys.* **A175**, 65 (1971)

[2] D.B.Adler and F.T.Adler, *Phys. Rev.* **C6**, 985 (1972).

[3] N.J.Pattenden and H.Postma, *Nucl. Phys.* **A167**, 225 (1971

[4] D.I. Tambovtsev, L.K. Kozlovsky, N.N. Gonin, N.S. Rabotnov, Yu.N. Kopach, A.B. Popov, W.I. Furman, J. Kliman, H. Postma, A.A. Bogdzel, and M.A. Guseinov, *Phys. At. Nucl.* **60/6**, 877 (1997).

[5] Yu.N.Kopach, A.B.Popov, W.I.Furman, N.N.Gonin, L.K.Kozlovsky, D.I.Tambovtsev, and J.Kliman, *Phys. At. Nucl.* **62/5**, 900 (1999)

[6] National Nuclear Data Center, Upton, NY, 11973-500, *http://www.nndc.bnl.gov.*

[7] R.Gwin, R.R.Spencer, R.W.Ingle, J.H.Todd, and S.W.Scoles, *Nucl. Sci. Eng.* **88**, 37 (1984)

[8] L.W.Weston and J.H.Todd, *Nucl. Sci. Eng.* **88**, 567 (1984).

[9] R.I.Schermer, L.Parsell, G.Brunhart, C.A.Reynolds, V.L.Sailor, and F.J.Shore, *Phys. Rev.* **167**, 1121 (1968).

[10] M.S.Moore, J.D.Moses, G.A.Keyworth, J.W.T.Dabbs, and N.W.Hill, *Phys. Rev.* **C18**, 1328 (1978).

[11] F.D.Brooks, J.E.Jolly, M.G.Schomberg, and M.G.Sowerby, AERE-M-1670 (1966).

[12] A.Michaudon, H.Derrien, P.Ribon, and M.Sanche, *Nucl. Phys.* **69**, 545 (1965).

[13] ENDF/B-VI Summary Documentation, ENDF-201 (BNL-17541), 1991.

[14] A.L.Barabanov and W.I.Furman, in *Proc. Int. Conf. on Nuclear Data for Science and Technology*, Gatlinburg, Tenessee, USA, May 9-13, 1994 ed.J.K.Dickens, p. 448; A.L.Barabanov and W.I.Furman, *Z. Phys.* **A357**, 411 (1997).

[15] A.Bohr, in *Proc. 1st Int. Conf. Peaceful Uses At. Energy*, Geneva, Vol. 2, p. 151 (1956).

[16] J.E.Lynn, "Theory of Neutron Resonance Reactions", (Claredon Press, Oxford, 1968).

[17] A.B.Popov, W.I.Furman, and L.Lason, in *Proc. of II Int. Workshop of Fission and Fission Fragment Spectroscopy*, edited by G.Fioni *et al.*, Seissyn, France, April 21-24, 1998, p. 349 (Woodbury, New York, 1998).

[18] Sh.S.Zeinalov *et al.*, in *Proc. VI Int. Sem. on Int. Neutr. with Nucl.*, Dubna, Russia, May 25-28 1999, p. 258 (Dubna, 1999).

[19] W.I.Furman and J.Kliman, in *Proc. 17th Int. Symp. on Nucl. Phys.*, Gaussig, 1987, p. 86 (Dresden, ZfK, 1988).

RELIABILITY OF MOSSES *(HYLOCOMIUM SPLENDENS, PLEUROZIUM SCHREBERI* AND *CALLIERGON GEGANTEUM)* AS BIOMONITORS OF HEAVY METAL ATMOSPHERIC DEPOSITION IN CENTRAL RUSSIA

M.V.Frontasyeva, Ye.V. Yermakova*, E. Steinnes**

FLNP, JINR, Dubna, Moscow Region, Russia

**L.N. Tolstoy Tula State Pedagogical University*

***Department of Chemistry, Norwegian University of Science and Technology, N-7491 Trondheim, Norway*

The moss biomonitoring technique was applied to study heavy metal atmospheric deposition in the area of Yasnaya Polyana, the memorial estate of L.N.Tolstoy, which is surrounded by numerous metallurgy, chemical, power, and machine-building plants in cities to the south of Moscow (Tula, Novomoskovsk, Schekino). This is the first time that a wide spectrum of heavy metals and other toxic elements was studied in the Tula Region.

Moss samples were collected in accordance with the sampling strategy adopted in the European Moss Survey on biomonitoring heavy metal atmospheric deposition [1]. In addition to standard epigeic moss species such as *Hylocomium splendens (Hs)* and *Pleurozium schreberi (Ps)*, the epiphytic moss *Calliergon geganteum (Cg)*, which is widely distributed at the given climatic conditions, was also studied.

Epithermal neutron activation analysis at the IBR-2 rector of FLNP made it possible to identify 38 elements in the moss samples including rare-earth elements, uranium, and thorium. Interspecies ratios of elements were calculated and compared to those observed by other investigators [2] in the Northern part of Europe at different environmental conditions. The interspecies ratio (*Ps:Hs*) varies between 1.10 and 1.50 for Mg, Ti, and Mn, whereas for Ca, Sc, Ni, Rb, Sr, In, La, Ce, Sm, Gd, Tb, Dy, Ta and Th it is less than 0.80. Because of living conditions in the relatively dry climate of the Tula Region,

Hylocomium splendens shows signs of degeneration in comparison with *Pleurozium schreberi* which is probably more resistent to dry climate. Pronounced differences in interspecies ratios were observed within the area under investigation for elements characteristic of air pollution, especially for V (*Ps:Hs* 1.39; *Ps:Cg* 1.35) and Sb (*Ps:Hs* 1.28; *Ps:Cg* 1.57). This suggests that interspecies variations depend mostly on deposition level. The interspecies ratios (*Ps:Cg*) varies from 0.80 to 1.20 for elements Mg, K, Ca, Cr, Mn, Fe, Co, Zn, As, Se, Br, Rb, Sr, Zr, Cd, In, Ba, Eu, W.

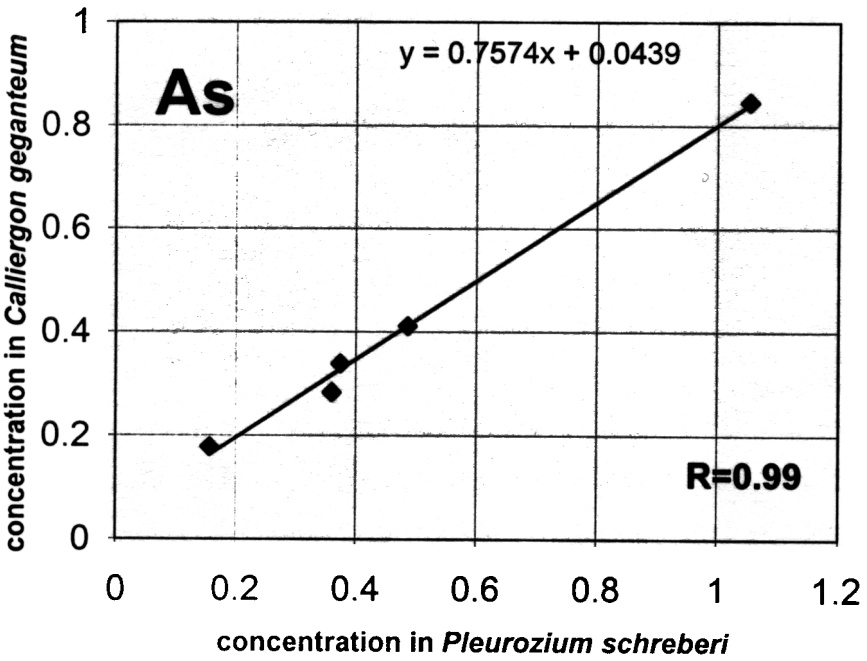

Fig 1. Concentration (ppm) of arsenic in Pleurozium schrebery versus Calliergon geganteum.

Based on this fairly extensive set of data where interspecies ratios vary within a relatively narrow range we conclude that the species *Calliergon geganteum* may replace the coventionally employed moss biomonitor species at sites where they are not found.

REFERENCES

[1] Åke Rühling. Heavy Metal Deposition in Europe – estimations based on moss analysis. Nordic Council of Ministers, Copenhagen, Nord 1994, p. 9.

[2] J.H. Hallereker, C. Reimann, P.de Catitat, T.E. Finne, G. Kashulina, H. Niskaavaara, I. Bogatyrev. Reliability of moss (Hylocomium splendens and Pleurozium schreberi) as a bioindicator of atmospheric chemistry in the Barents region: Interspecies and field duplicate variability. The Science of the Environment 218 (1998) 123-139.

SELECTION OF APPROPRIATE MOSS BIOMONITORS FOR STUDYING ATMOSPHERIC ELEMENTAL DEPOSITION IN CHINA

O. A. Stan, Zh. H. Zhang*, M.V. Frontasyeva, E. Steinnes**

FLNP, JINR, Dubna, Moscow Region, Russia

**IHEP, CAS, Beijing, China*

***Norwegian University of Science and Technology, Trondheim, Norway*

The moss biomonitoring is a well established technique widely used to study atmospheric deposition in Nordic countries [1] and in the Western Europe [2]. The present work is the first attempt to apply this technique to some areas of China. Twelve different moss species were collected during the autumn of 1998. Most of the samples were taken from highly polluted areas within the Beijing Region. The remaining ones were collected from the national park in Tianmu Mountain, Zhejiang Province, South-East China. The purpose of the present study is to find appropriate moss biomonitors growing in China, as alternatives to the species *Hyloconium splendens (HS)* and *Pleurozium schreberi (PS)* adopted in the European Moss Survey [3] which unfortunately are not found in the Beijing Region (see Table 1).

Table 1 Name and location of the Mosses in China

Name	Site	Name	Site
Myuroclada maximoviczii	BR	*Taxiphyllum taxirameum*	BR
Oxystegus cylindricus	BR	*Brachythecium plumosum*	BR
Brachythecium plumosum	BR	*Grimmia pilifera*	BR
Entodon rubicundus	BR	*Bryhnia sublaevifolia*	NP
Platyhypnidium riparioides	BR	*Entodon cf. seductrix*	NP
Taxiphyllum taxirameum	BR	*Oxyrrhynchium savatier*	NP

BR = Beijing Region; NP = National Park

A total of 49 elemental concentrations were determined by nuclear and related analytical techniques: epithermal neutron activation analysis (ENAA) at the IBR-2 reactor of JINR; hydride-generation atomic fluorescence spectrometry (HGAFS) and flame and/or graphite furnace atomic absorption spectrometry at IHEP.

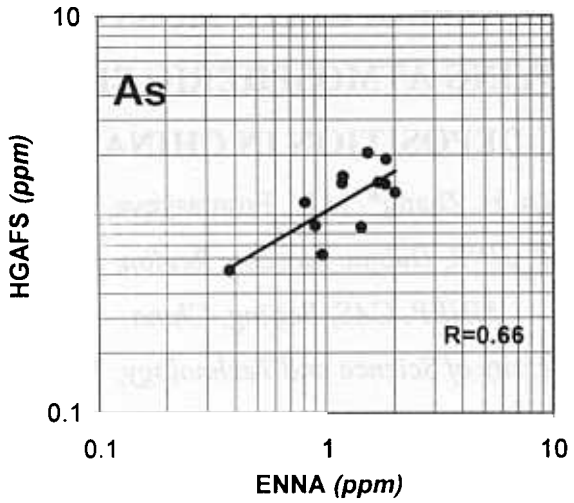

Fig.1. Arsenic concentrations in mosses obtained by ENAA versus HGAFS

A comparison of the results obtained by ENAA and HGAFS for arsenic is shown in Fig. 1. Quality assurance for element determination was provided by using IAEA standard reference material Lichen IAEA-336 in both laboratories.

In spite of the fact that all 12 moss species reflect the general level of pollution in entirely different regions of China (Fig.3), two moss species *Myuroclada maximoviczii* and *Entodon rubicundus* demonstrated the best ability to substitute each other by showing the highest correlation (Fig.2).

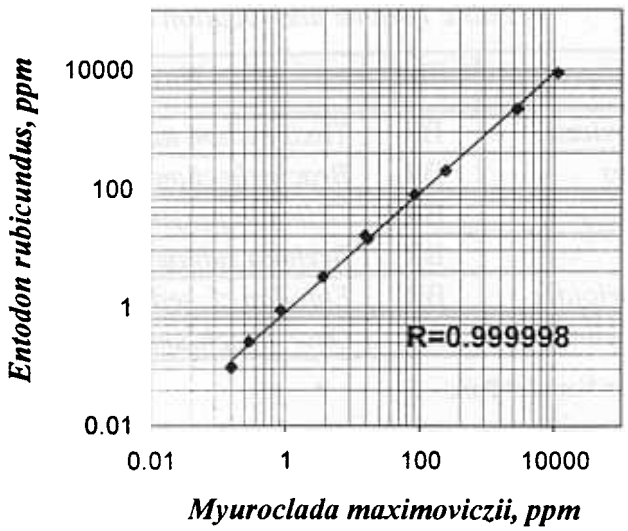

Fig 2. Comparison Myuroclada maximoviczii versus Entodon rubiundus

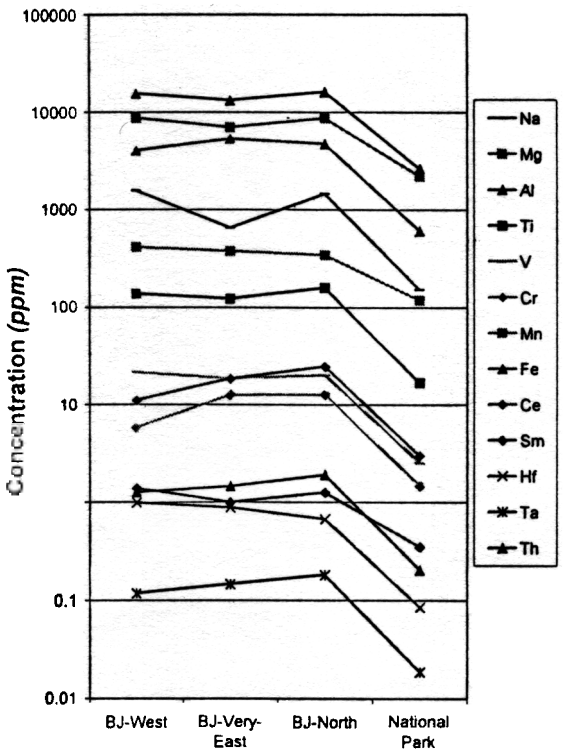

Fig. 3 Some elemental concentrations in mosses from the Beijing Region and the National Park in South-East China

Practically for all elements the concentrations are about 10 times lower in the National Park than at other sampling sites

The results obtained encourage us to plan an extended moss survey for assessment of air pollution in urban and rural areas of China.

REFERENCES

[1] M.V. Frontasyeva, E. Steinnes, Epithermal Neutron Activation Analysis of Mosses Used to Monitor Heavy Metal Deposition Around an Iron Smelter Complex, Analyst, 120 (1995) 1437-1440

[2] B. Markert, O. Wappelhorst, V. Weckert, U. Herpin, U. Siewers, K. Friese, G. Breulmann, The Use of Bioindicators for Monitoring the Heavy-Metal Status of the Environment, *J. Radioanal. Nucl. Chem.*, 240 (1999) 425-429

[3] Å. Rühling, Atmospheric Heavy Metal Deposition in Europe - estimations based on moss analysis., Nordic Council of Ministers, *NORD 1994:9* (1994) 10-13